Heritage Science

RESEARCH

Open Access

New insights on the analysis of the causes of glossy lustre on the surface of ancient Chinese bronze mirrors

Yunpeng Wang[1,2], Shasha Long[1], Xuening Wang[1,2], Fangzhi Liu[2] and Qinglin Ma[3*]

Abstract

Ancient Chinese bronzes, particularly bronze mirrors, often develop a fatty, oily, or greasy film on their surface, known as patina. This film can appear silvery, green, or black. Bronze mirror samples from the Spring and Autumn Period (770–476/403 BCE) to the Ming Dynasty (1368–1644 CE) were analyzed using a systematic approach that included super depth of field three-dimensional microscopy, scanning electron microscopy/energy dispersive X-ray spectroscopy (SEM–EDS), Raman spectroscopy, and THM-Py-GC/MS. The analysis indicates the presence of advanced organic acid lead in the matrix of ancient bronze mirrors. The ancient existence of the lost wax method combined with the mould method of bronze casting technology is verified through simulation experiments and ancient literature. Ancient bronze mirrors may have utilized this technique, with advanced organic acid lead remaining in the mirror mould that entered the bronze mirror matrix during pouring. The Lead organic acids in bronze mirrors readily precipitate on the surface and cover the mirror. The change in the greasy sheen on the surface of the bronze mirror may be related to the degree of corrosion. If the mirror's corrosion level is low, the organic acid lead film remains transparent. If the level of corrosion is significant, the organic acid lead film may darken in color due to oxidation, aging, hydrolysis, or microbial activity.

Keywords High-tin bronze mirror, Black patina, Silvery patina, Advanced organic acid lead, Lost wax

Introduction

Ancient bronze mirrors often have an oily sheen on their surface. This sheen is referred to as 'slivery patina' if it is bright and silvery, 'green patina' if it is emerald green, and 'black patina' if it is black. 'Patina' bronze mirrors are a type of bronze mirror with a smooth, greasy sheen and a jade-textured surface. Most research has concentrated on the 'black patina' and 'silvery patina'. Currently, there are two primary explanations for this phenomenon: artificial treatment mechanisms and natural corrosion mechanisms. however, due to the limitations of these explanations, the causes of the greasy film on the bronze surface have not been adequately explained [1–17]

According to a study, the greasy sheen on the surface of jade is caused by advanced fatty acid salts within the jade, which come from sedimentary organic matter in the original rock [18]. Several studies have analyzed the organic materials present in the bronze mirror mould. Hiroshi Araki [19] discovered a substance resembling beeswax in a mould of a Warring States mirror. This discovery led him to conclude that there was a tradition of casting mirrors in ancient China using the lost-wax method. Ceramic mirror moulds from the Han Dynasty were discovered at the Linzi City site in Qi State. These moulds have a black carbonic layer on the surface of the

*Correspondence:
Qinglin Ma
qinglinma226@126.com
[1] Joint International Research Laboratory for Environmental and Social Archaeology of Shandong University, Qingdao 266237, China
[2] Shandong Provincial Cultural Relics Conservation, Restoration and Identification Center, Jinan 250014, China
[3] School of Materials Science and Engineering, Beijing University of Chemical Technology, Beijing 100029, China

cavity, sprue, and exhaust channel. Yang [20] suspected that a layer of beeswax or a similar substance was applied to the inside of the mirror mould as a release agent before casting. Wang [21]discovered a black coating layer on the moulds derived from the Houma foundry. The coating material was identified as either wax or animal fat.

The author is involved in the preservation of cultural artifacts in Shandong. Before conservation or restoration, it is necessary to analyze cultural objects. A section of the bronze was cut off, embedded in epoxy resin, sanded with sandpaper, and polished with 0.25 um emery polish to examine the cross-section of the specimen. Under fortuitous circumstances, the author discovered organic materials growing out of the matrix of the bronze mirror samples after weeks of storage in metal sample cabinets. This was an unusual phenomenon compared to other types of bronze samples stored in the same environment. The author examined hundreds of bronze artifact samples stored in metal cabinets. Only 10 bronze mirror samples, 1 bronze tripod sample, 1 bronze Zhou vessel sample, and 1 bronze Dou vessel sample exhibited a similar pattern. The author polished some of the samples and altered the storage environment. However, the new organic material still precipitated after a few weeks, indicating that the organic material in the bronze samples was not caused by external contamination. Additionally, the fact that one of the bronze tripod samples was newly excavated by the Archaeological Institute in 2018 eliminates the possibility that the organic matter came from conservation material or environmental contamination of the collection [22].

This paper utilizes the super depth of field three-dimensional microscope, scanning electron microscopy/energy dispersive X-ray spectroscopy (SEM–EDS), Raman spectroscopy (LCRS), and THM-Py-GC/MS to investigate the morphology and chemical composition of the organic material. The objective of this research is to offer a plausible explanation for the formation of the greasy sheen surface of bronze mirrors.

Experimental procedure

Samples

Samples of ancient bronze artefacts were collected from Jinan Museum (JN), Ju County Museum (JZ), Shandong Institute of Cultural Relics and Archaeology (SICRA), and Confucius Museum (CM). The bronzes nominally cover the Spring and Autumn Period (770–476/403 BCE), the Han Dynasty(206 BC to 220 CE), the Tang Dynasty(618–907 CE), and the Song (960–1279 CE) and Ming (1368–1644 CE) dynasties. The bronze mirror samples were classified into three categories. Six mirrors had a silver patina (Fig. 1, JN06, JN88, JN68, JN10, JZ24, JN46), two mirrors had a black patina (Fig. 1, JZ09, JZ12), and two mirrors had a dark green patina (Fig. 1, JZ03 and JZ11). Table 1 and Fig. 1 provide further details on the samples.

Analytical techniques

The polished cross-sectional samples were examined using a Leica DVM6 three-dimensional microscope with super depth of field.

The micromorphology and chemical composition of the micro-areas were characterized using Phenom XL scanning electron microscopy, with EDAX Genesis 2000XMS energy dispersive X-ray spectroscopy. The analyses were conducted in a low vacuum environment (60 Pa) using an operating voltage of 15 kV.

Phase components were characterized using laser micro-confocal Raman spectroscopy (Renishaw invia) with a research-grade Leica microscope with a spatial resolution of less than 0.5 μm. The optical objectives used were 50×and 100×, and the laser wavelength was 785 nm.

THM-Py-GC/MS: The EGA/PY-3030D tube furnace pyrolyzer (Frontier Lab, Inc.) was set at a pyrolysis temperature of 550 °C and coupled to a gas chromatography-mass spectrometer (Agilent, 8860-5977B, Frontier feed). The Py/GC interface temperature was 300 °C and the pyrolysis products were separated and characterized using a gas chromatograph-mass spectrometer. Chromatographic conditions: using a capillary column model Ultra-ALLOY ± 5 (Frontier Lab, 30 m × 0.25 mm × 0.25 μm, stationary phase of 5% phenyl—95% methyl polysiloxane); the carrier gas used was helium (He, purity 99.999%). The column flow rate was 1.0 mL/min. The shunt injection ratio was 2:1. The chromatographic conditions were as follows: the initial temperature of the oven was set at 40 ℃ for 2 min, followed by a gradient of 6 ℃/min up to 300 ℃ for 9 min. The quadrupole mass spectrometer was set at 150 ℃ for detection, the temperature of the MS transmission line is 300 ℃, the ionization mode is EI source (ion source voltage 70 eV), ion source temperature 230 ℃, full scan mode, mass number range 33 ~ 600 amu, solvent delay is 3 min.

Due to the small amount of organic material precipitated from the sample, it was necessary to scrape the material together with the alloy matrix and place it in the sample cup. Following this, 3 μl of methylation reagent (tetramethylammonium hydroxide, McLean) were added.

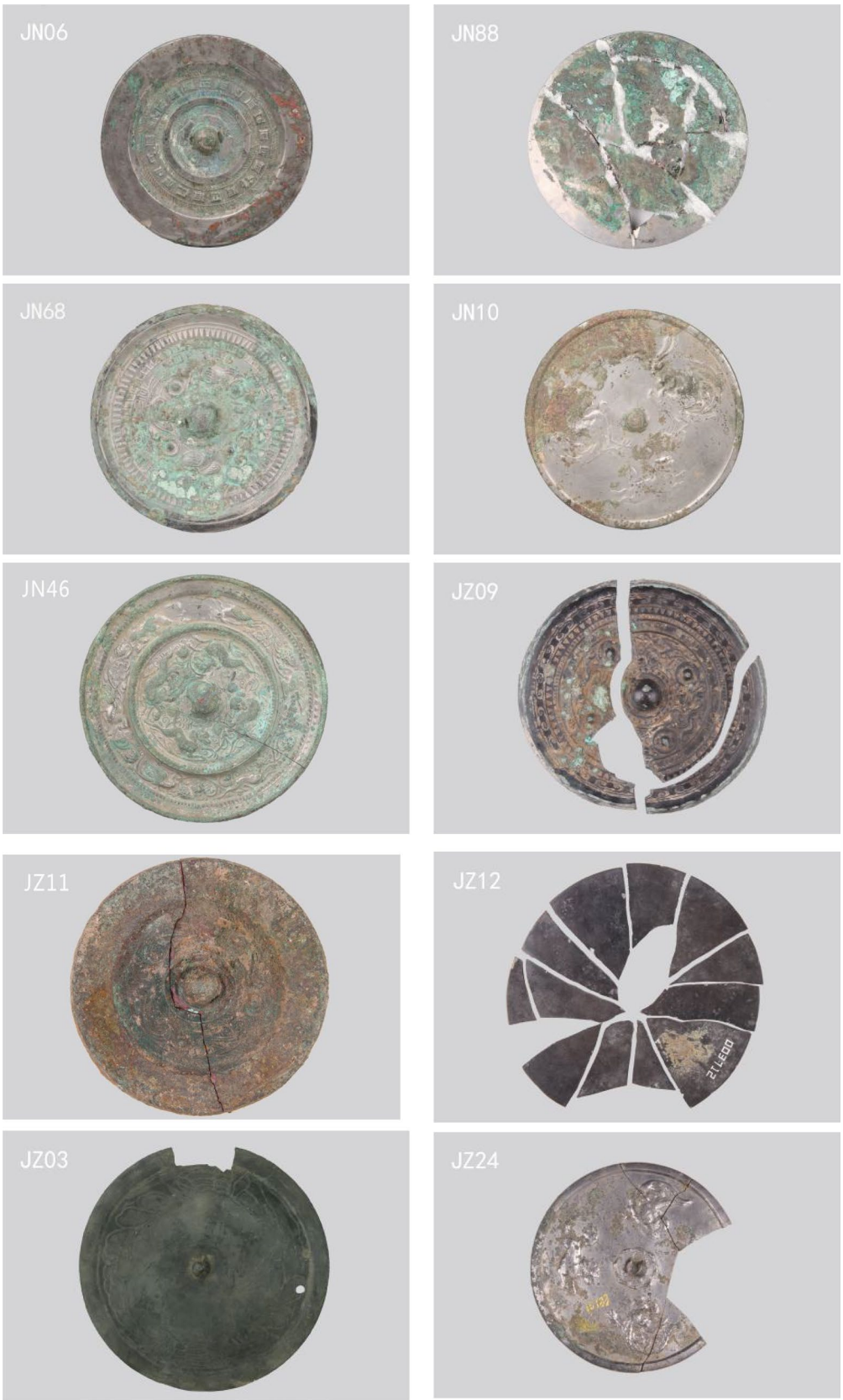

Fig. 1 Photos of the bronze mirrors derived from the JN, the JZ (SICRA and CM only sent samples, no photographs of the artefacts)

Table 1 Description of the bronze artifacts derived from the JN, the JZ, the SICRA, and the CM

Sample	Artifact Name	Feature	Dynasty	Origin
JN06	Zhao Ming mirror (昭明镜)	Fragment of bronze with silvery patina	Western Han	Jinan Museum
JN88	"Jian Ri Zhi Guang"' with Grass Leaf Pattern mirror (见日之光单层草叶纹铜镜)		Western Han	
JN68	Four Beasts and Four Nodules Pattern mirror (四乳四禽纹镜)		Eastern Han	
JN10	Two Phoenixes and Two Beasts mirror (双鸾双兽纹镜)		Tang	
JN46	Auspicious beast and rare bird and grape pattern mirror (瑞兽珍禽葡萄纹铜镜)		Tang	
JZ09	Four Beasts and Four Nodules Patterns with Inscription mirror (四兽四乳铭文镜)	Fragment of bronze with black patina	Han	Ju Country Museum
JZ12	Persimmon with Arc and Inscription mirror (柿蒂连弧铭文镜)		Han	
JZ69	Persimmon and Four Nodules Patterns and Four Beasts with Inscription mirror (柿蒂四乳神兽铭文镜)		Han	
JZ11	Four Beasts and Dragon pattern mirror (四乳夔龙纹铜镜)	Fragment of bronze with dark green patina	Han	
JZ03	Three Beasts mirror (三兽镜)		Tang	
JZ24	Stone Beast mirror (石兽镜)	Fragment of bronze with silvery patina	Song	
LG16	bronze Tripod (鼎)	Fragment of bronze	Spring and Autumn Period	Shandong Provincial Institute of Cultural Relics and Archaeology (Unearthed in 2018 at Wangfutai Cemetery, ancient city of Lu state, Qufu)
KZ24	Bronze Zhou (舟)	Fragment of bronze lid	Spring and Autumn period	Confucius Museum
KZ67	Bronze Dou (豆)	Fragment of bronze	Ming	

Results

Composition of the bronze artifact samples matrix

Table 2 presents the results of the EDS analysis of the uncorroded areas in the matrix of freshly prepared bronze samples, all of which were ternary copper-lead–tin alloys. The tin content of most samples ranged from 16.6 to 29.3 wt%, with KZ67 having the lowest tin content of 4.6 wt%. The lead content of most samples ranged from 2.7 to 15.8 wt%, with LG16 having the highest lead content of 24.5 wt%.

Table 2 Chemical composition of the bronze samples analyzed by EDS (Wt %)

Sample	Cu	Sn	Pb	Fe	As
JN06	71.0	24.9	4.1	—	—
JN88	68.0	24.1	7.9	—	—
JN68	70.1	24.6	5.3	—	—
JN10	67.4	23.3	9.3	—	—
JN46	66.8	26.7	6.5	—	—
JZ09	69.0	25.2	5.8	—	—
JZ11	67.1	26.8	6.1	—	—
JZ12	68.0	29.3	2.7	—	—
JZ03	74.0	17.0	9.0	—	—
JZ24	67.3	24.6	7.0	0.6	0.5
LG16	58.9	16.6	24.5	—	—
KZ24	71.2	17.1	11.7	—	—
KZ67	79.6	4.6	15.8	—	—

Morphology and composition of the organic materials

Micro-morphological observation

Based on the Leica microscope analysis in Fig. 2, the strip material growth on the cross-section of the bronze mirrors appears white and translucent. Figure 3 shows SEM/backscattered electron (BSE) images of specimens JN06, JN68, JN10, JN46, JZ09, JZ11, JZ12, JZ03, JZ24, LG16, KZ24, and KZ67, indicating that the white strip material growth is mainly present on the non-corroded matrix area. A small amount of black oily material was also observed on some of the sample profiles.

SEM/backscattered electron (BSE) images of sample JN88 in Fig. 4 reveal that the white lead phase was

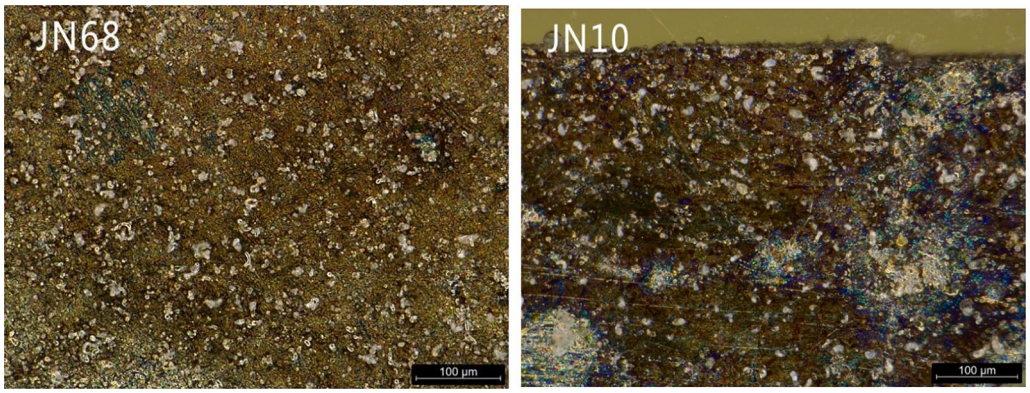

Fig. 2 Morphology of white strip materials of sample JZ68 and JN10 cross-sections

exposed after wiping the white strip materials with alcohol. This indicates that the white strip materials are mostly grown from the lead phase.

In Fig. 5, SEM(BSE) images of bronze artifact samples show the morphology of the white strip materials at high magnification. The selected area of Sample JZ12 is the corrosion area, while the selected area of all other samples is the bronze matrix. Table 3 presents the results of the energy spectrum analysis, where X denotes the white strip materials and H denotes the black oil materials. The α-phase and δ-phase contents were consistent with theoretical values, and the bronze substrate did not corrode. The N and O elements have been subtracted from the EDS data, and the relative content of the C element is still indicative although it is affected by the low vacuum environment in the SEM. According to the EDS analysis, the white strip materials have a high lead content, and the carbon content is significantly higher than the bronze matrix (which is about 2%). This may be due to the presence of some kind of organic lead salt. The black oil material has a high content of carbon, copper, and tin, which is probably some kind of organic salt of copper.

Raman spectral analysis

Figure 6 shows the Raman spectra of white strip materials precipitated in three samples (JZ03, JZ09, and JZ24) collected from the JZ Museum. The spectra of the samples are similar to each other, and the results indicate that they are consistent with the lead of fatty acid. The peak at 2851 cm^{-1} represents the stretching vibration of the CH_2 and CH_3. A peak at 1441 cm^{-1} was assigned to $c\leqslant^{o}_{o}$ symmetric bond stretching vibration peaks formed after the homogenization of carbonyl groups in carboxylates. A peak at 1296 cm^{-1} corresponds to the $(CH_2)_n$ non-planar oscillation. This is followed by several peaks between 1062 cm^{-1} and 1129 cm^{-1} corresponding to C–C skeletal telescopic vibrations. The C–C–C symmetric stretching vibration of carbon chains in the region of 890 cm^{-1} [23].

Figure 7 shows the Raman spectra of white strip materials precipitated in five samples (JN06, JN10, JN46, JN68, and JN88) collected from the JN museum. Some of the spectral peaks in the samples were similar to those of the JZ sample, but there were also other characteristic peaks present. The stretching vibration of the C=C bond has a peak at 1651 cm^{-1}. A peak at 1601 cm^{-1} coincides with the stretching vibration of the benzene ring, and the 1001 cm^{-1} is attributed to the respiratory vibration of the benzene ring [24]. The Raman spectra of the white materials precipitated in bronze artifact samples collected from the CM and the WF are similar to those of the JN samples, as shown in Fig. 8.

THM-Py-GC/MS analysis

Since the methylation reagents added to the samples tend to react with carboxylates to form esters, the pyrolysis products are mostly higher fatty acid-converted esters (Fig. 9, Table 4) the main ingredient is hexadecanoic acid or dilute acid esters). Some aromatic compounds were also present in some samples. Based on the results of THM-Py-GC/MS analysis and Raman spectroscopy, it can be concluded that the white stripe materials growing on the bronze matrix are advanced organic acid lead. The materials from JZ samples consist mostly of saturated fatty acid lead, while the materials from JN samples consist mostly of unsaturated fatty acid lead and aromatic acid lead.

Simulation experiment

Advanced organic acids are solids at room temperature. Similar materials do not exist in laboratory environments, and it is difficult for similar components in the soil to penetrate the uncorroded bronze matrix. Therefore, organic lead acid growths on the matrix of bronze artifacts are not formed by environmental pollution.

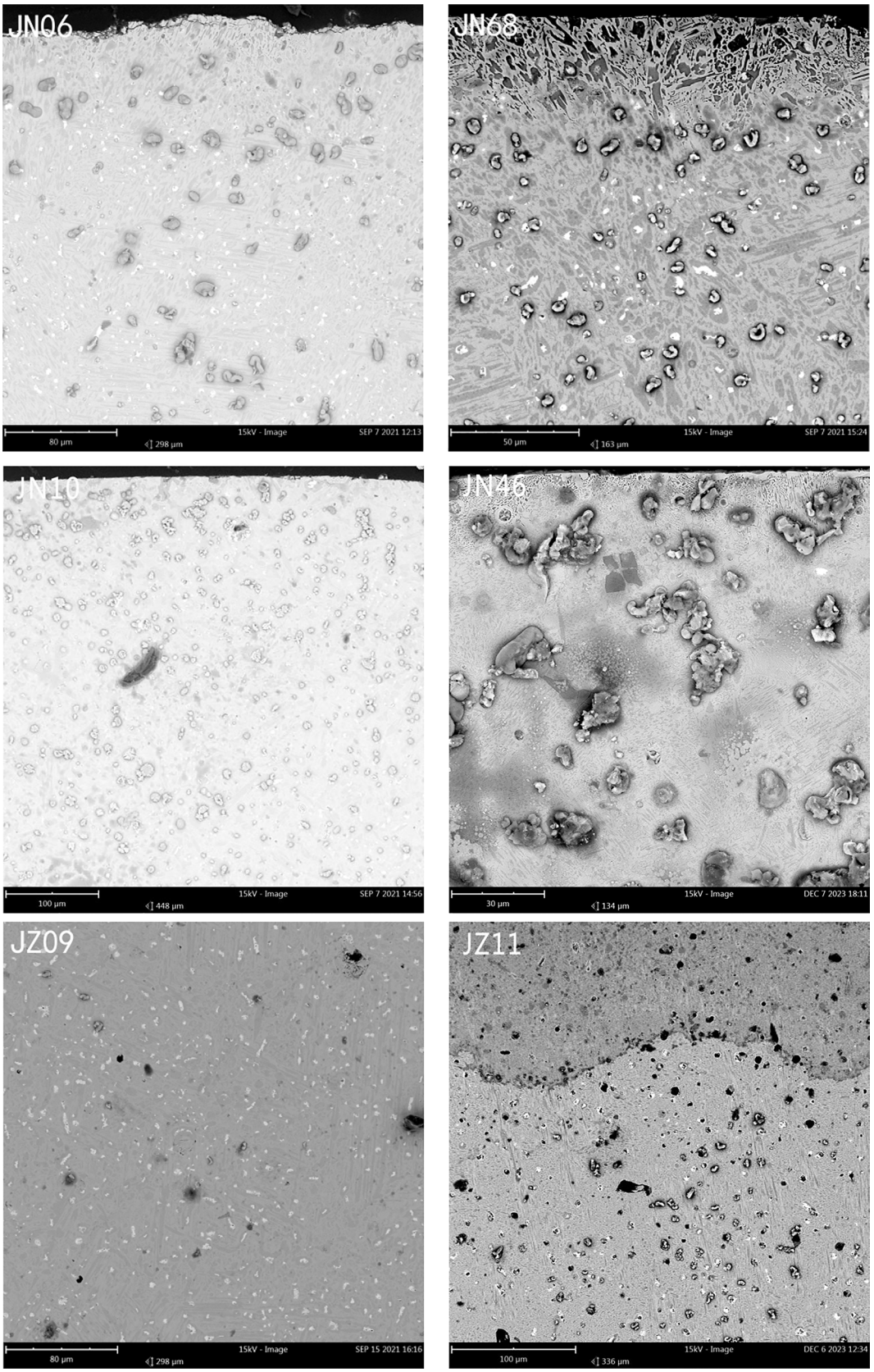

Fig. 3 SEM/backscattered electron (BSE) images of white strip materials growth on the bronze artifacts samples

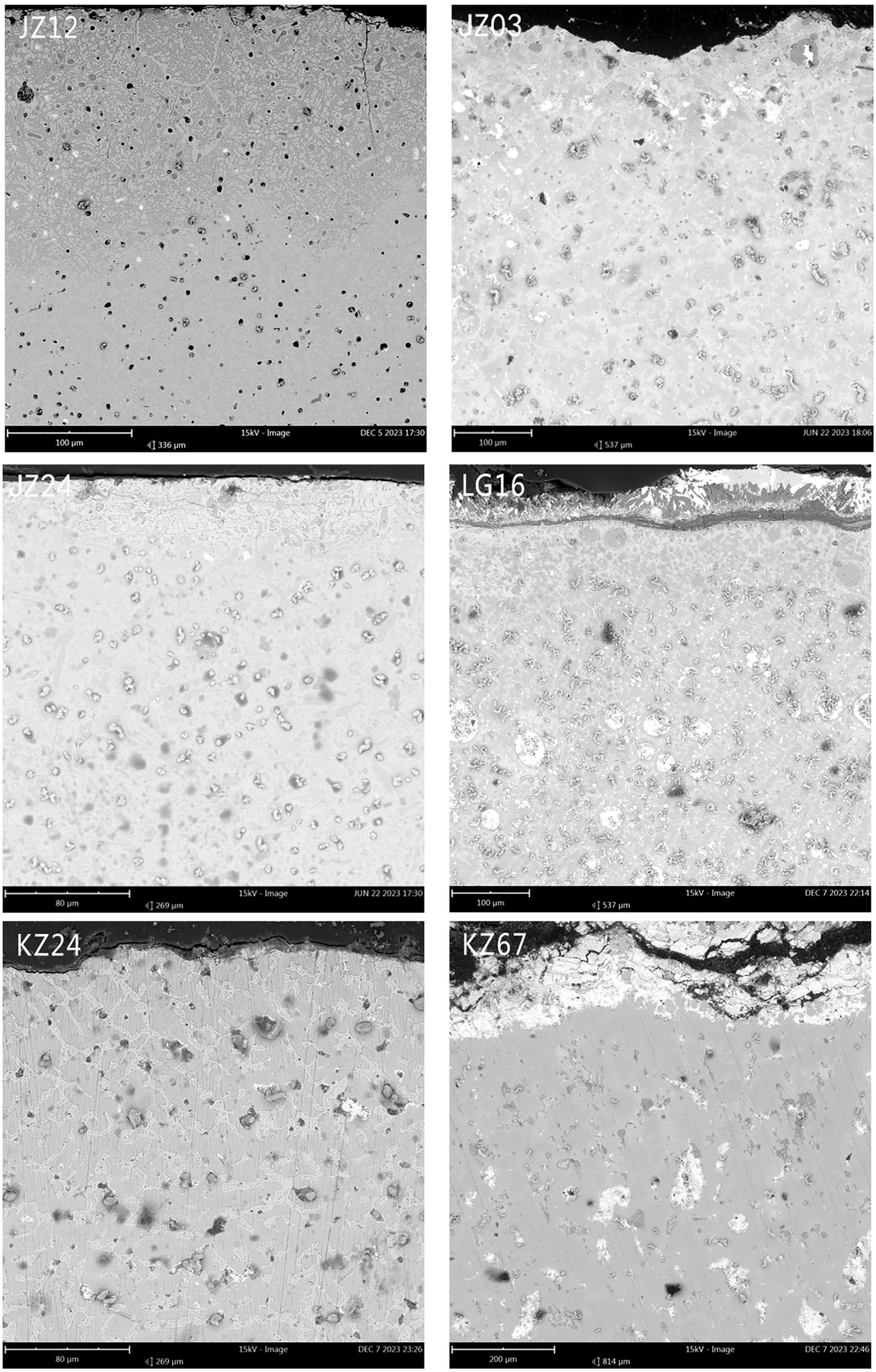

Fig. 3 continued

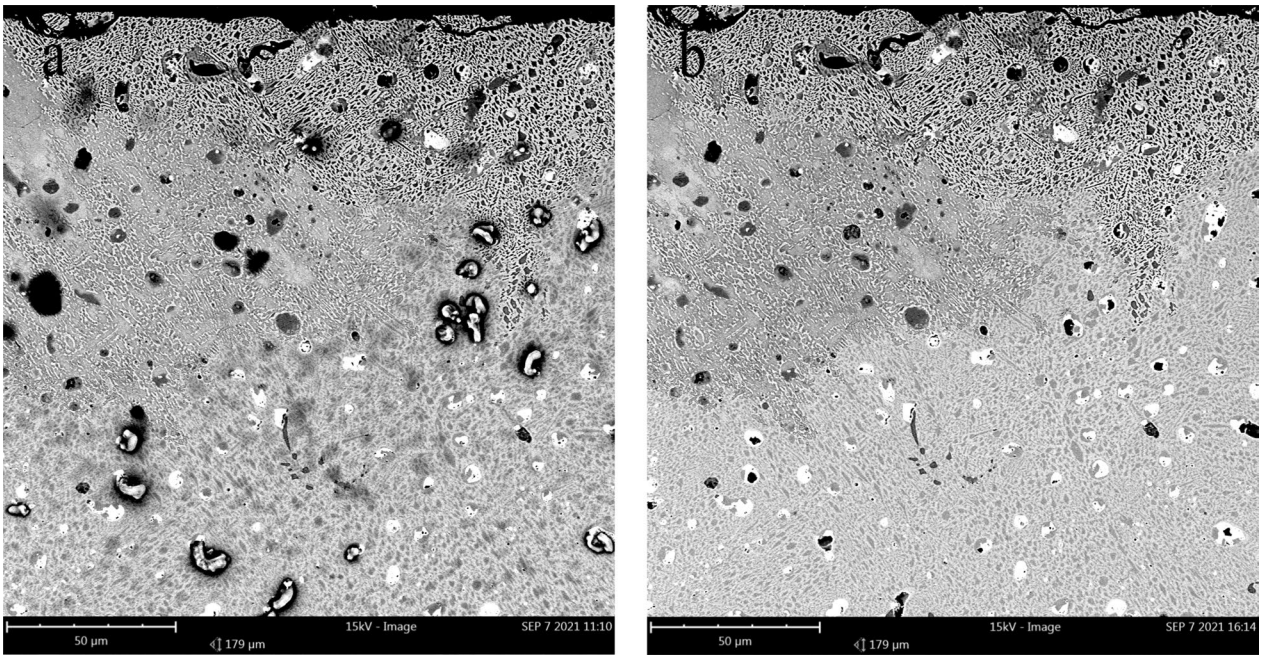

Fig. 4 SEM (BSE) images of white strip materials growth on sample JN88 cross-sections (**a**: the organic materials growth on the matrix; **b**, the organic materials were wiped by alcohol)

Similarly, if the surface of a bronze mirror had been sealed with lead soap, the lead soap would not be able to penetrate the uncorroded bronze matrix. Therefore, the lead soap in the bronze mirror has nothing to do with modern or ancient conservation treatments.

When bronze is melted at high temperatures, the added organic material burns off or evaporates and cannot remain in the metal. The organic lead acid in the bronze mirror should originate from residue on the casting. If organic matter, such as grease or beeswax, is present in the casting mould, it may react with the metallic lead in the copper solution to form advanced organic acid lead during casting. To verify this speculation, analytically pure stearic acid was heated to a liquid state (70 ℃), and added a lead block. The black lead oxide on the surface of the lead block dissolved and expressed a silver color, after which the reaction stagnated. The weight loss of the lead blocks was 0.34%. The experiment was repeated with other types of fats and oils, and the results were the same. The metallic lead did not react with the advanced organic acids or esters. This suggests that the residue in the mould during casting should be the prepared advanced organic acid lead.

To test the method of melting advanced organic acid lead into the bronze mirror, the inside of the plaster mould was coated with a 1 mm thick layer of lead stearate, which was 3–4 mm thick at the bottom. The copper-tin melt without lead was then poured into the plaster mould. The lead stearate was ignited at a high temperature vaporized and evaporated quickly. The surface of the formed No.1 copper block was free of residual lead stearate, but the bottom was greatly irregular due to the boiling washout of lead stearate. An area of approximately 0.7 mm in the bottom of the No. 1 copper block contained a small amount of lead stearate, while the matrix had no lead (Fig. 10, Table 5). Upon enlarging the lead-containing area of the No. 1 copper block, it was observed that the majority of the lead stearate existed as fine white particles within the (α + δ) eutectoid. The results suggest that the presence of a few lead stearates in the mirror mould may result in its incorporation into the bronze mirror matrix during the casting process. However, the amount is insufficient to penetrate deeply Table 5.

In the second experiment, a significant amount of lead stearate was added to the plaster mould. However, it was observed that the copper-tin melt cooled rapidly as it was poured, causing it to solidify before it could fill the mirror mould. Lead stearate, which has a specific heat capacity greater than that of oil and less than that of water, is an excellent coolant. Therefore, the poured copper-tin melt lost heat too quickly and solidified completely after only slightly penetrating the mirror mould. Figure 11 displays the SEM(BSE) image of the cross-section of the No.2 copper block. The image shows that the white lead stearate was only present on the surface of the No.2 copper

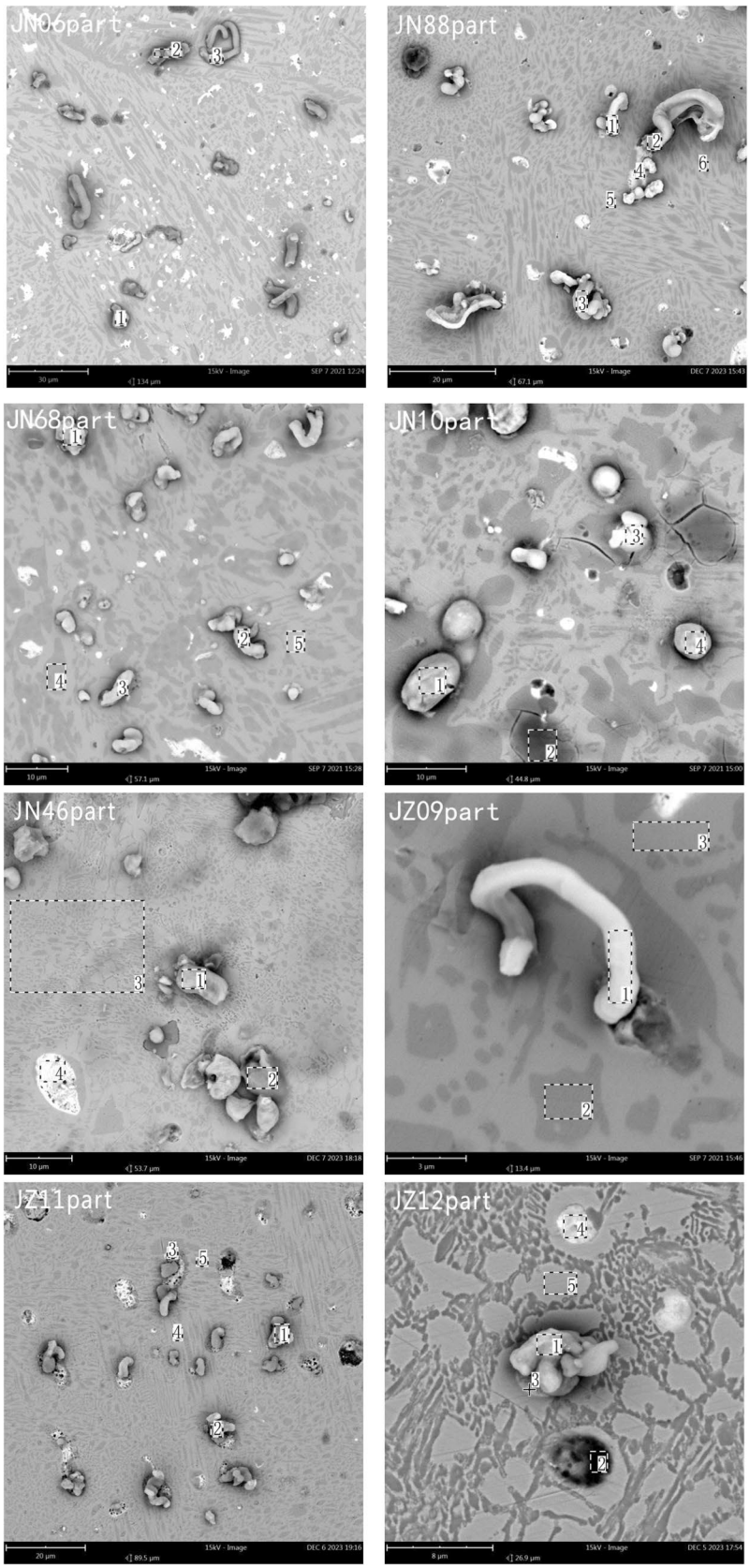

Fig. 5 SEM(BSE) images of white strip materials growth on bronze artifacts samples

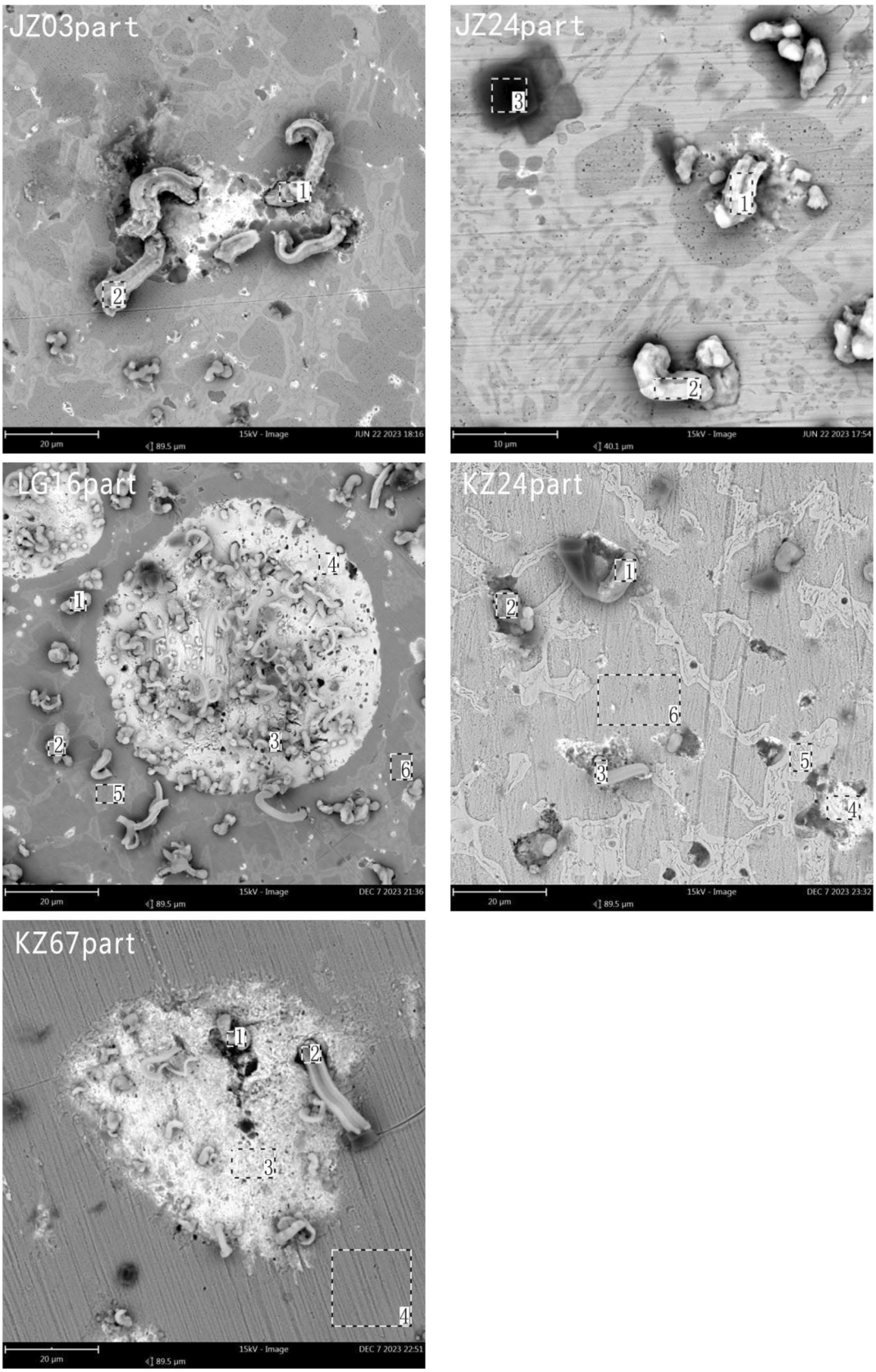

Fig. 5 continued

Table 3 Chemical composition (Wt %) of the bronze artifacts samples analyzed by EDS

Sample	Area	Phase	Cu	Sn	Pb	C	Si	Al	Na	K	Ca	Fe	Mg	S	Cl	As
JN06 part	1	X	24.6	9.9	57.2	7.7	0.3	0.3	—	—	—	—	—	—	—	—
	2	X	23.8	9.9	58.7	7.1	0.2	0.3	—	—	—	—	—	—	—	—
	3	X	27.3	8.7	57.9	5.7	0.2	0.1	—	—	—	—	—	—	—	—
JN88 part	1	X	19.1	7.7	67.9	4.7	0.4	0.2	—	—	—	—	—	—	—	—
	2	X	32.8	8.9	50.9	7.0	0.1	0.3	—	—	—	—	—	—	—	—
	3	X	23.9	9.9	57.7	8.0	0.1	0.3	—	—	—	—	—	—	—	—
	4	Pb	15.5	4.4	77.6	2.2	0.2	0.1	—	—	—	—	—	—	—	—
	5	δ	65.0	29.7	2.6	2.2	0.3	0.2	—	—	—	—	—	—	—	—
	6	α	72.4	20.0	4.4	2.8	0.2	0.1	—	—	—	—	—	—	—	—
JN68 part	1	X	17.7	6.6	67.1	7.9	0.4	0.3	—	—	—	—	—	—	—	—
	2	X	23.4	10.3	58.2	7.3	0.5	0.3	—	—	—	—	—	—	—	—
	3	X	32.5	9.3	53.6	4.3	0.2	0.2	—	—	—	—	—	—	—	—
	4	α	77.3	16.9	2.5	3.3	—	—	—	—	—	—	—	—	—	—
	5	δ	65.2	29.6	2.7	2.5	—	—	—	—	—	—	—	—	—	—
JN10 part	1	X	15.4	4.8	73.2	6.0	0.3	0.4	—	—	—	—	—	—	—	—
	2	H	46.5	14.1	19.8	5.1	0.9	0.4	4.5	0.6	0.4	3.9	0.5	3.0	0.4	—
	3	X	15.8	4.1	75.8	3.4	0.6	0.3	—	—	—	—	—	—	—	—
	4	X	20.6	7.9	63.7	7.3	0.2	0.3	—	—	—	—	—	—	—	—
JN46part	1	X	11.0	5.5	71.8	11.1	0.2	0.4	—	—	—	—	—	—	—	—
	2	X	11.5	4.9	70.9	12.2	0.2	0.3	—	—	—	—	—	—	—	—
	3	α + δ	61.3	27.9	3.7	6.3	0.2	0.3	—	—	—	—	—	—	0.3	—
	4	Pb	6.4	2.7	87.0	3.6	0.2	0.1	—	—	—	—	—	—	—	—
JZ09 part	1	X	33.8	14.0	40.8	10.5	0.1	0.8	—	—	—	—	—	—	—	—
	2	α	79.6	17.7	1.6	1.1	—	—	—	—	—	—	—	—	—	—
	3	δ	65.8	30.4	2.8	1.0	—	—	—	—	—	—	—	—	—	—
JZ11 part	1	X	24.7	10.2	54.9	9.4	0.3	0.5	—	—	—	—	—	—	—	—
	2	X	18.3	7.2	61.5	12.1	0.3	0.6	—	—	—	—	—	—	—	—
	3	Pb	15.3	5.4	76.8	2.2	0.1	0.2	—	—	—	—	—	—	—	—
	4	δ	66.6	30.5	1.8	1.1	—	—	—	—	—	—	—	—	—	—
	5	α	76.8	19.7	2.1	1.4	—	—	—	—	—	—	—	—	—	—
JZ12 part	1	X	10.9	7.8	71.7	8.9	0.3	0.4	—	—	—	—	—	—	—	—
	2	H	25.1	17.3	43.4	13.6	0.4	0.2	—	—	—	—	—	—	—	—
	3	Pb	42.0	25.2	30.0	2.5	0.2	0.1	—	—	—	—	—	—	—	—
	4	Pb	16.7	11.5	68.1	3.2	0.4	0.2	—	—	—	—	—	—	—	—
	5	δ	61.5	33.6	2.5	1.8	0	0.2	—	—	—	—	—	—	—	—
JZ03 part	1	X	14.6	4.1	75.4	5.3	0.1	0.4	—	—	—	—	—	—	—	—
	2	X	20.1	6.2	66.7	6.3	0.2	0.5	—	—	—	—	—	—	—	—
JZ24 part	1	X	15.0	4.8	72.5	7.0	0.2	0.5	—	—	—	—	—	—	—	—
	2	X	16.1	7.3	67.7	7.0	0.3	0.5	—	—	—	1.0	—	—	—	—
	3	H	52.9	10.7	3.2	5.4	0.4	0.4	—	—	—	12.0	—	13.7	0.2	1.3
LG16 part	1	X	14.8	4.1	75.7	4.8	0.2	0.4	—	—	—	—	—	—	—	—
	2	X	22.1	7.1	64.0	6.0	0.2	0.6	—	—	—	—	—	—	—	—
	3	X	7.2	2.1	82.9	6.9	0.3	0.6	—	—	—	—	—	—	—	—
	4	Pb	5.3	1.9	90.6	2.0	0.2	0.2	—	—	—	—	—	—	—	—
	5	α + δ	65.7	25.0	6.8	2.2	0.1	0.2	—	—	—	—	—	—	—	—
	6	α	76.3	14.3	6.6	2.5	0.1	0.2	—	—	—	—	—	—	—	—

Table 3 (continued)

Sample	Area	Phase	Cu	Sn	Pb	C	Si	Al	Na	K	Ca	Fe	Mg	S	Cl	As
KZ24 part	1	X	18.6	4.0	64.4	11.0	1.7	0.3	—	—	—	—	—	—	—	—
	2	X	19.7	3.8	63.1	8.3	4.7	0.3	—	—	—	—	—	—	0.3	—
	3	X	15.8	4.0	74.6	4.7	0.7	0.2	—	—	—	—	—	—	—	—
	4	Pb	10.5	0.8	81.3	2.2	1.6	0.2	—	—	—	—	—	—	3.4	—
	5	α + δ	65.2	28.3	4.0	2.0	0.4	0.1	—	—	—	—	—	—	—	—
	6	α	75.8	12.8	7.7	2.6	0.5	0.1	—	—	—	—	—	—	0.5	—
KZ67 part	1	X	10.9	0.7	81.7	5.9	0.5	0.3	—	—	—	—	—	—	—	—
	2	X	11.0	0.5	80.0	7.9	0.2	0.4	—		—		—		—	—
	3	Pb	6.9	0.4	89.6	1.9	0.5	0.3	—		—		—		—	0.4
	4	α	85.2	3.9	5.7	2.4	0.4	0.3	—		—		—		—	2.1

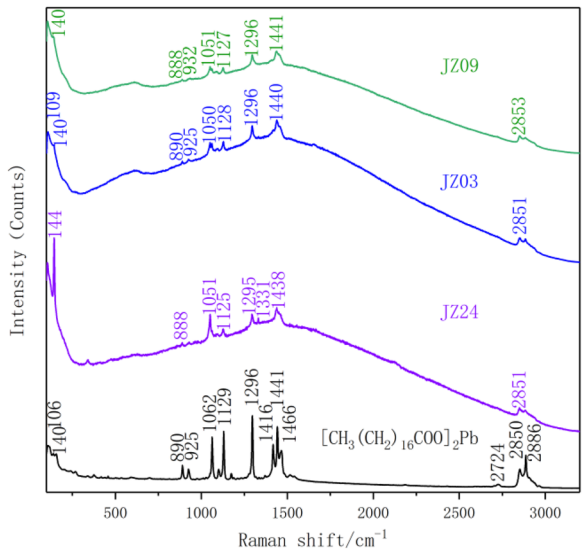

Fig. 6 Raman spectra image of JZ samples

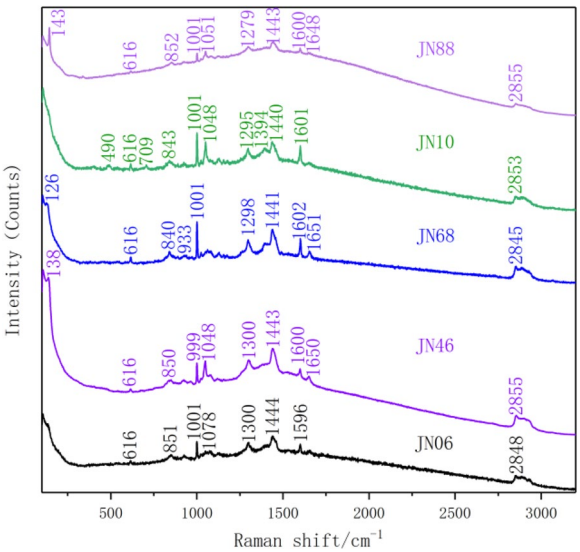

Fig. 7 Raman spectra image of JN samples

block. This result suggests that the amount of lead stearate in the mirror mould can not be excessive before casting Table 6.

During the second experiment, the lead stearate in the mould was occasionally ignited during casting. The flame was extinguished when the copper-tin melt completely blocked the gate. It was found that small amounts of lead stearate were present in this kind of copper block matrix (Fig. 12, No. 3 copper block). The metallographic structure of the No. 3 copper block consists of the δ phase and (α + δ) eutectic, with the lead stearate mostly present in the δ phase. The metallographic structure of the No. 1 copper block consists of the α-phase and (α + δ) eutectoid. The lead stearate is mainly present in the distribution area of the eutectic

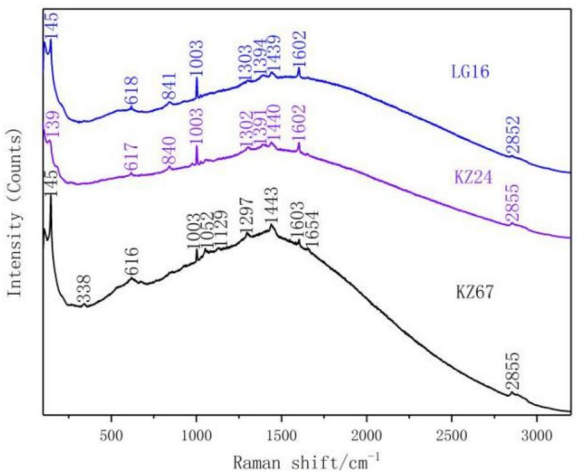

Fig. 8 Raman spectra image of CM and WF samples

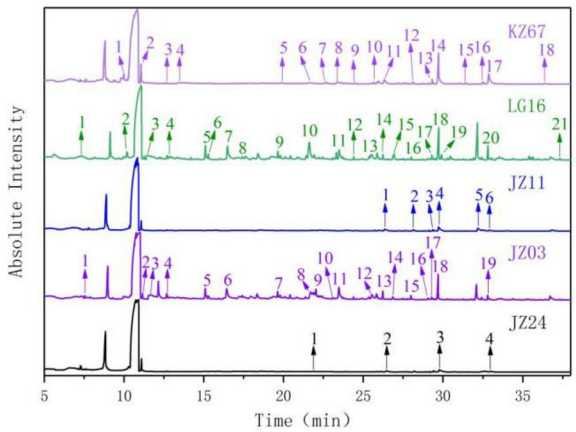

Fig. 9 The chromatogram of sample KZ67, LG16, JZ11, JZ03, and JZ24 obtained by THM-Py-GC/MS analysis

(Fig. 10). The melting point of each organization of the bronze alloy decreases with an increase in tin content. The α phase has the highest melting point, followed by the (α + δ) eutectoid, and the δ phase has the lowest melting point. Organic acid Lead is more prone to occur in low melting point phases, so advanced organic acid lead in ancient bronze mirrors is mostly found in lead (The melting point of metallic lead is only 327 ℃) (Table 7).

To allow lead stearate to penetrate the bronze mirror matrix, the low-melting organization in bronze must remain in a liquid state for an extended period. A wax cake, measuring approximately 40 mm in diameter and 8 mm in thickness, was moulded from lead stearate. The wax cake is encased vertically in refractory plaster, leaving a sprue and riser. Before casting, the mould is baked, causing some of the lead stearates to liquefy and flow out. Approximately 20 ~ 30% of the lead stearates remain in the muold due to their high viscosity. The copper-tin melt was poured into the mould, and the lead stearate quickly boiled and burned. Smoke blackened the gypsum moulding cavity and sprue as the flame burned, forming the No. 4 copper block in about a minute. Figure 13 shows that there is no lead stearate on the surface of the No. 4 copper block, but the white lead stearate is present throughout the entire bronze matrix which has a morphology similar to that of granular lead found in ancient bronze mirrors (Table 8).

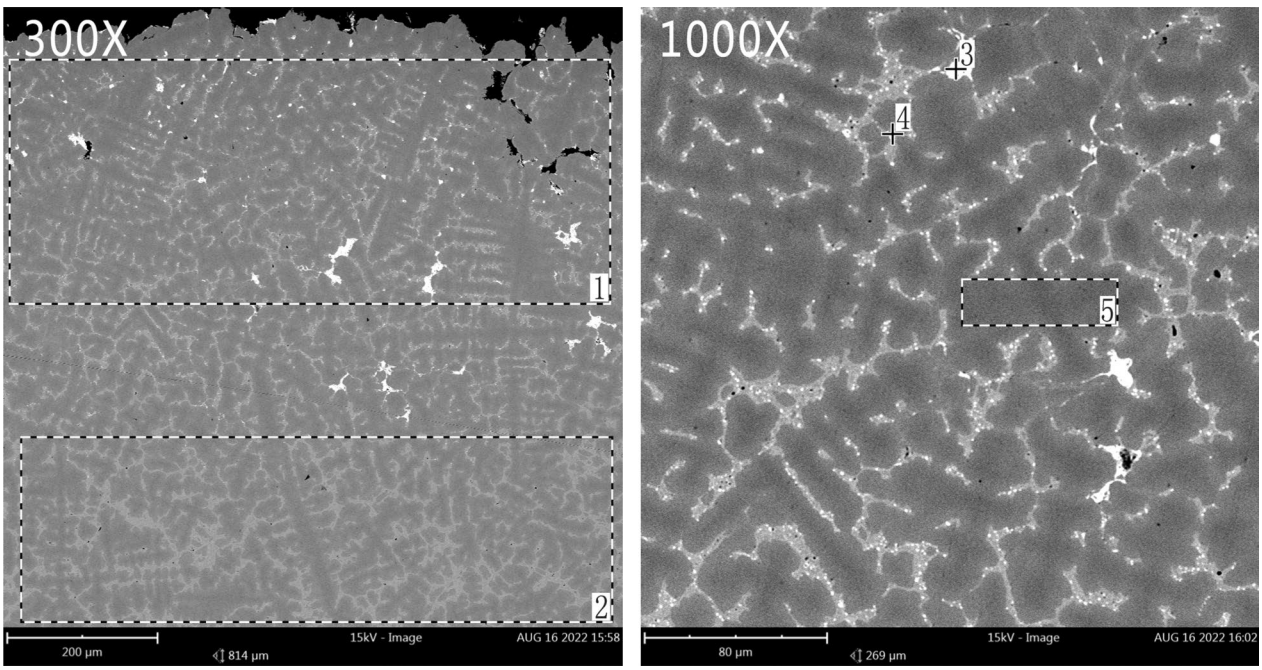

Fig. 10 SEM/backscattered electron (BSE) images of cross-section sample of No. 1 copper block

Table 4 The main compounds identified in sample KZ67, LG16, JZ11, JZ03, and JZ24 by THM-Py-GC/MS (the peak No. corresponding to Fig. 9)

Sample	Peak No	RT	Area%	Formula	Compounds identified
KZ67	1	9.80	0.364	$C_8H_{14}O_2$	n-Butyl methacrylate
	2	11.15	0.086	$C_8H_{14}O_2$	Methyl 6-heptenoate
	3	12.66	0.13	$C_{11}H_{22}$	1-Undecene
	4	13.44	0.234	$C_8H_8O_2$	Methyl benzoate
	5	19.86	0.161	$C_{14}H_{28}$	1-Tetradecene
	6	21.59	0.428	$C_{10}H_{18}O_4$	Dimethyl octoate
	7	22.66	0.342	$C_{13}H_{26}O_2$	Methyl laurate
	8	23.36	0.303	$C_{11}H_{20}O_4$	Dimethyl azelate
	9	24.51	0.067	$C_{14}H_{28}O_2$	Methyl tridecanoate
	10	25.96	0.468	$C_{15}H_{28}O_2$	Methyl myristate
	11	26.33	1.361	$C_{15}H_{30}O_2$	Methyl myristate
	12	28.12	0.321	$C_{16}H_{32}O_2$	Methyl pentadecanoate
	13	29.32	0.384	$C_{17}H_{32}O_2$	Methyl (Z)-7-hexadecenoate
	14	29.41	0.143	$C_{17}H_{32}O_2$	Methyl (Z)-7-hexadecenoate
	15	31.43	0.181	$C_{18}H_{36}O_2$	Methyl heptadecanoate
	16	32.49	0.187	$C_{19}H_{36}O_2$	Methyl 11-octadecenoate
	17	32.86	2.656	$C_{19}H_{38}O_2$	Methyl stearate
	18	35.97	0.057	$C_{21}H_{42}O_2$	Methyl 18-methylnonadecanoate
LG16	1	7.30	0.552	C_9H_{18}	1-Nonene
	2	9.97	0.206	$C_{10}H_{20}$	1-Decene
	3	11.42	0.647	C_6H_6O	Phenol
	4	12.72	0.259	$C_{11}H_{22}$	1-Undecene
	5	15.10	1.237	$C_{12}H_{24}$	1-Dodecene
	6	15.28	0.419	$C_{12}H_{26}$	Dodecane
	7	16.04	0.063	$C_8H_{10}O$	4-Ethylphenol
	8	17.42	0.103	$C_{13}H_{26}$	1-Tridecene
	9	19.64	0.597	$C_{14}H_{28}$	1-Tetradecene
	10	21.61	3.133	$C_{12}H_{26}O$	1-Dodecanol
	11	23.83	0.119	$C_{16}H_{34}$	Cetane
	12	24.40	0.187	$C_{13}H_{24}O$	Methyl-6, 8-dodecenyl ether
	13	25.55	0.635	$C_{15}H_{30}O_2$	Methyl myristate
	14	26.23	0.37	$C_15H_{30}O_2$	Methyl myristate
	15	26.88	0.309	$C_{24}H_{46}O_3$	Eicosylpropen-2-yl carbonate
	16	28.01	0.164	$C_{16}H_{32}O_2$	Methyl pentadecanoate
	17	29.30	0.356	$C_{17}H_{32}O_2$	Methyl (Z)-7-hexadecenoate
	18	29.74	0.222	$C_{17}H_{34}O_2$	Methyl palmitate
	19	30.45	0.457	$C_{20}H_{42}O_3$	Cetyl methyl
	20	32.82	0.964	$C_{19}H_{38}O_2$	Methyl stearate
	21	37.34	0.09	$C_{21}H_{44}O$	Dodecyl nonyl ether
JZ11	1	26.45	0.332	$C_{15}H_{30}O_2$	Methyl myristate
	2	28.20	0.182	$C_{16}H_{32}O_2$	Methyl pentadecanoate
	3	29.41	0.13	$C_{17}H_{32}O_2$	Methyl (Z)-7-hexadecenoate
	4	29.79	0.856	$C_{17}H_{34}O_2$	Methyl palmitate
	5	32.59	0.134	$C_{19}H_{36}O_2$	Methyl (E)-9-octadecenoate
	6	32.96	0.157	$C_{19}H_{38}O_2$	Methyl stearate

Table 4 (continued)

Sample	Peak No	RT	Area%	Formula	Compounds identified
JZ03	1	7.32	0.586	C_9H_{18}	1-Nonene
	2	11.29	0.019	$C_8H_{10}O$	1-Methoxy-4-methylbenzene
	3	11.71	2.381	C_6H_{6O}	Phenol
	4	12.67	0.261	$C_{11}H_{22}$	1-Undecene
	5	15.09	0.942	$C_{12}H_{24}$	1-Dodecene
	6	16.25	0.104	$C_8H_{10}O$	4-Ethylphenol
	7	19.63	0.475	$C_{14}H_{28}$	1-Tetradecene
	8	21.70	1.749	$C_{12}H_{26}O$	1-Dodecanol
	9	22.18	0.275	$C_{16}H_{30}O_2$	Z-3-Tetradecen-1-yl acetate
	10	23.68	0.189	$C_{16}H_{32}$	1-Hexadecene
	11	23.82	0.138	$C_{16}H_{34}$	Hexadecane
	12	25.54	0.962	$C_{16}H_{30}O_2$	N-dodecyl methacrylate
	13	26.22	0.589	$C_{15}H_{30}O_2$	Methyl myristate
	14	26.85	0.299	$C_{17}H_{32}O_3$	Carbonic acid 1-en-2-yl tridecyl ester
	15	27.99	0.355	$C_{16}H_{32}O_2$	Methyl pentadecanoate
	16	29.05	0.162	$C_{17}H_{34}O_2$	Methyl palmitate
	17	29.28	0.175	$C_{17}H_{32}O_2$	Methyl (Z)-7-hexadecenoate
	18	29.70	2.166	$C_{17}H_{34}O_2$	Methyl palmitate
	19	32.81	0.382	$C_{19}H_{38}O_2$	Methyl stearate
JZ24	1	21.85	0.023	$C_{17}H_{36}O$	2-Methyl-1-cetyl alcohol
	2	26.34	0.536	$C_{15}H_{30}O_2$	Methyl myristate
	3	29.73	1.15	$C_{17}H_{34}O_2$	Methyl palmitate
	4	32.90	0.157	$C_{19}H_{38}O_2$	Methyl stearate

Discussion

Evidence of lead soap occurrence

Advanced Organic Acid Lead, also known as Lead Soap, is formed when lead oxides react with saturated or unsaturated fatty acids found in animal fats or vegetable oils. Lead Soap production technology has been present in China for a long time. The literature records 'Lead paste' (铅膏) in Zhouhou Beiji Fang (《肘后备急方》) during the Jin Dynasty (266–420 CE). According to the given text, the process involves taking thirteen taels of clear sesame oil or vegetable oil and seven taels of lead oxide into an iron pan and frying on a simmer, with coarse wet willow branches grating and churning until the color turns black. The fire should then be strengthened while still fanning the fan and churning. When the smoke breaks off, it indicates that the lead paste is finished preparation.

Table 5 Chemical composition (Wt %) of the No.1 copper block cross-section sample analyzed by EDS

Area	Cu	Sn	Pb	C
1	82.9	12.6	3.3	1.2
2	85.0	14.4	—	0.6
3	12.1	2.8	82.5	2.6
4	17.5	3.5	73.5	5.6
5	90.1	9.0	—	0.9

During casting, the Lead Soap applied to the inner surface of the mould in small amounts would evaporate quickly and vaporize or burn out at high temperatures, it is difficult to retain and penetrate the bronze matrix. Therefore, it is improbable that the Lead Soap originated from a mould release agent. The literature titled 'The Exploitation of the Works of Nature' (《天工开物》), written in 1637, records a casting technique that combines the moulding cast method and the lost wax method. According to the text, the method for casting bronze bells and tripods weighing more than ten thousand pounds is the same. First, a pit more than ten feet

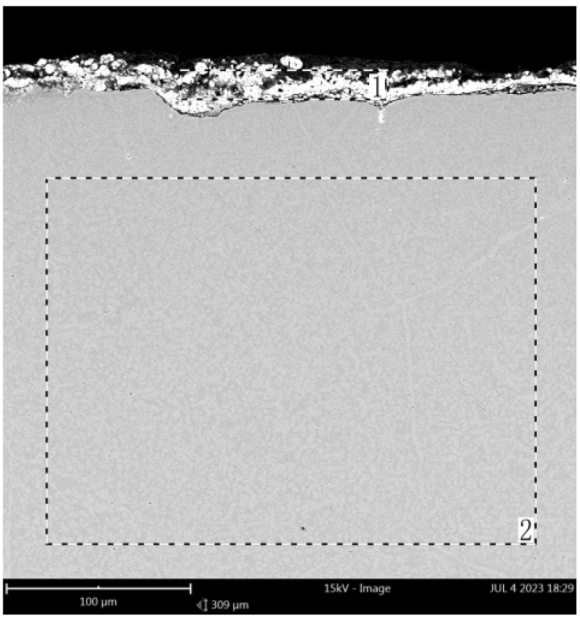

Fig. 11 SEM/backscattered electron (BSE) images of cross-section sample of No. 2 copper block

Table 6 Chemical composition (Wt %) of the No.2 copper block cross-section sample analyzed by EDS

Area	Cu	Sn	Pb	C
1	7.6	4.5	82.4	5.5
2	71.0	28.0	—	1.0

deep is dug and kept dry. Then, it is constructed as if it were a house. To create the inner mould, lime, fine sand, and clay are blended into the soil and moulded without any cracks. Once dry, a coating of butter and yellow wax, with a ratio of eight-tenths tallow and two-tenths yellow wax, is applied to the top few inches. Finally, a tall roof is constructed to protect the bell model from the sun and rain, especially during summer when the oils and waxes may not solidify easily. After applying a smooth layer of oil wax with a plasterer's knife, the surface can be carved with various words and patterns. Next, a mixture of finely pounded clay powder and charcoal powder is applied layer by layer on top of the oil wax, creating a coating that is a few inches thick. When the inside and outside of the outer mould are naturally dry and solid, roast it slowly on top of a fire. This will cause the oil wax inside to dissolve and flow cleanly from the opening of the mould. The cavity between the inner and outer moulds will become the place where the bells and tripods will be moulded in the future. It takes ten pounds of copper to fill the void for every pound of oil and wax vacated.

Based on the mentioned documents, it is known that during the Ming Dynasty, oil and wax were applied to the outside of the inner mould to facilitate the engraving of fine patterns on the wax film when making bronze bells and tripods. Fine clay was then applied to the outside of

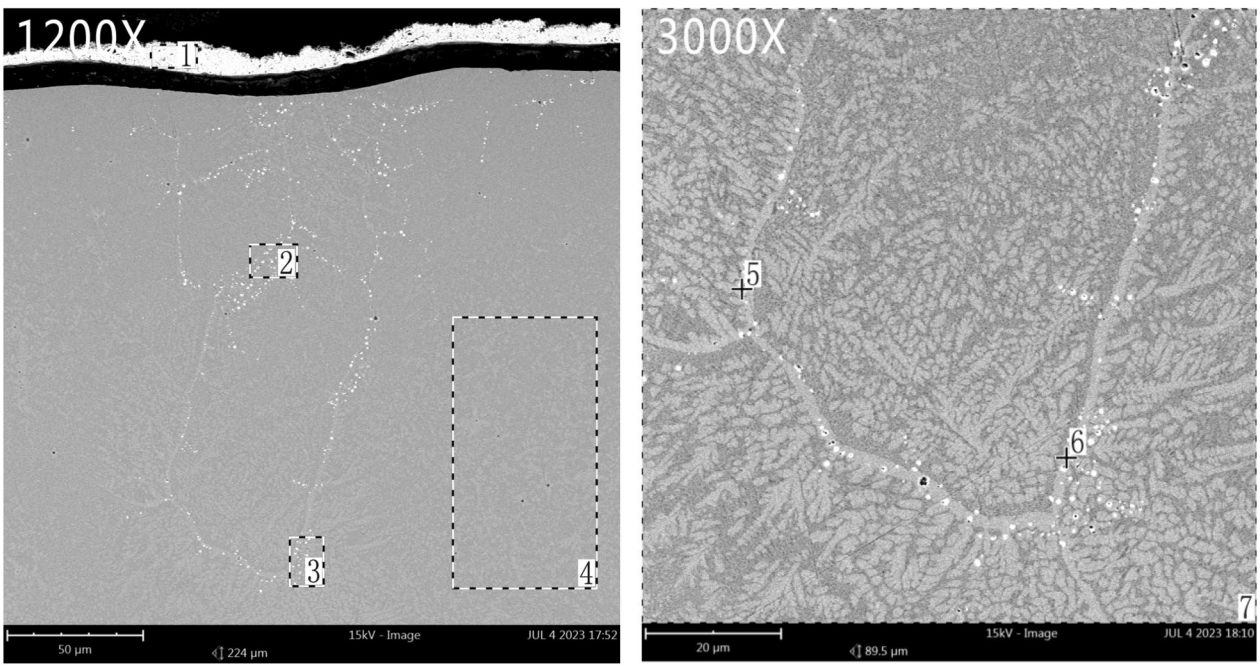

Fig. 12 SEM/backscattered electron (BSE) images of cross-section sample of No. 3 copper block

Table 7 Chemical composition (Wt %) of the No.3 copper block cross-section sample analyzed by EDS

Area	Cu	Sn	Pb	C
1	4.5	2.5	88.1	4.9
2	65.4	26.1	6.8	1.7
3	66.9	28.0	3.8	1.3
4	71.5	27.1	—	1.4
5	48.9	25.9	21.5	3.7
6	47.9	24.7	24.0	3.4
7	69.8	27.9	1.0	1.3

the wax film to create the outer mould. The casting technique used for Bronze Ding LG16 was likely similar to this process. Additionally, the literature notes that oil wax is too soft and prone to melting when used as a raw material for wax film. The Lead Soap melting point around 100 ℃ and moderate hardness are ideal for wax film raw materials. There are fine decorations on the surface of the bronze mirror, and it is probably also used a combination of fan casting and lost wax casting. During the casting process, the remaining lead soap in the Fan is completely melted and ignited, leaving the low melting point metal in a liquid state for an extended period. Subsequently, the lead soap flows into the bronze matrix along with the molten liquid metal. Lead Soap has been found in bronze artifacts from the Spring and Autumn Period to the Ming Dynasty in Shandong Province, suggesting that this combined bronze casting technology may have been widely used.

Effects of lead soap

Metals expand and contract with temperature changes. Lead Soap is soft and can easily precipitate and accumulate on the surface of copper mirrors as the metal contracts. The presence of Lead Soap inevitably affects the surface luster of copper mirrors. Bronze mirrors often have an oily sheen due to the white, translucent, waxy solid with a greasy sheen that is Lead Soap. The organic acid salts have excellent corrosion resistance, so ancient bronze mirrors are usually well preserved.

Organic matter can deepen in color due to oxidation, aging, hydrolysis, or microbial activity. Heat may accelerate this process. When buried in soil, bronzes are susceptible to galvanic corrosion. Electrochemical corrosion, also known as a corrosion cell, is essentially a short-circuited primary cell. Batteries are designed based on this principle. When a battery is short-circuited, the electrical energy is completely converted into heat and released. In severe cases, the battery may even spontaneously combust. Metals corrode slowly, and the conversion of electrical energy to heat is also a slow process. The silvery patina mirror corrosion degree is light (corrosion layer thickness is generally less than 50 μm), and senior organic acid lead maintains a transparent state. Black patina mirror corrosion degree is heavier (corrosion layer thickness

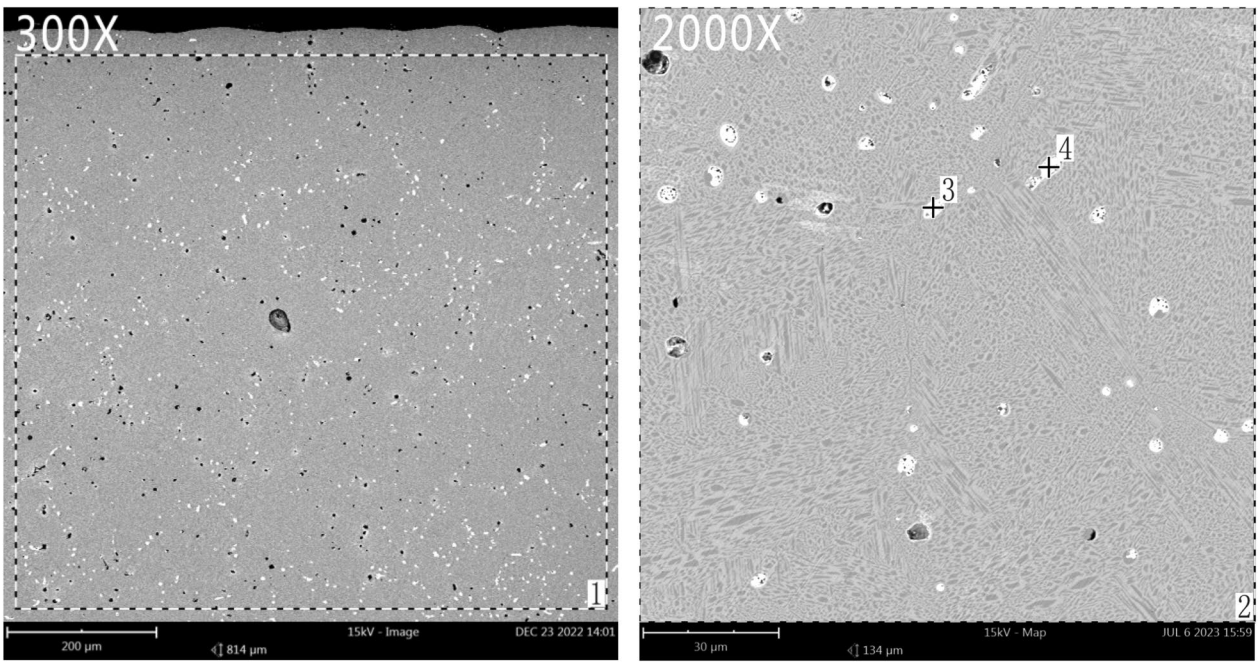

Fig. 13 SEM/backscattered electron (BSE) images of cross-section sample of No. 4 copper block

Table 8 Chemical composition (Wt %) of the No. 4 copper block cross-section sample analyzed by EDS

Area	Cu	Sn	Pb	C
1	70.4	26.4	2.5	0.7
2	70.6	27.0	1.9	0.5
3	10.6	4.5	71.8	13.1
4	8.9	3.7	74.5	12.9

is generally greater than 150 μm), and corrosion that lasts for thousands of years has the potential to deepen the lead soap color on the surface of bronze mirrors.

Difficulty of detection

Organic components are rarely tested for in metals. The amount of lead soap present in bronze mirrors is typically low and mixed with metallic lead, which can make it challenging to detect. The conversion of lead soap on bronze mirror surfaces to organic acids in acidic environments can be challenging to detect when mixed with soil components in the rust layer. Due to the glassy state of Lead Soap after heating, conventional rock and mineral identification methods such as X-ray diffraction and microscopic laser Raman spectroscopy (with very strong fluorescence) are not effective in identifying it. XRF and EDX analyses often subtract elements such as C, O, and N as air constituents. In FTIR, the characteristic main peaks of organic acid salts are covered by the bending vibration peaks of the O–H bond of the water of crystallization, and the characteristic peaks such as methyl and methylene are often misidentified as humic acid. This is likely the reason why Lead Soap has not been detected in bronze mirrors thus far.

Conclusions

This study found that white striations, confirmed to be Lead Soap, precipitated from the cross-section of bronze mirror samples preserved at room temperature. The Lead Soap in the bronze mirror should have remained in the mould during casting. Since small amounts of organic materials in the mould tend to vaporize and evaporate or burn out completely when poured at high temperatures, the possibility of its use as a release agent is ruled out. Simulation experiments have shown that when using the lost wax method to make bronze, the lead soap as moulding material will be partially retained in the mould during the process of heating. During pouring, the high temperature generated by burning lead soap keeps the low-melting-point tissues in the bronze mirrors in a liquid state for an extended period, and the lead soap can flow into the bronze matrix along with the liquid metal melt. According to the ancient literature "The Exploitation of the Works of Nature", there is a casting technique that combines the lost wax method with the moulding method. Ancient bronze mirrors may have used a similar technique and used lead soap as the raw material for the lost wax process.

Lead Soap is soft, and after precipitation on the surface of the copper mirror is easy to diffuse and cover the copper mirror (artificial wiping can also make it cover the whole object), which would form a corrosion-resistant layer. Electrochemical corrosion is the most common process of bronze corrosion in nature. During this process, the temperature of the corrosion layer would rise slightly due to the heat energy coming from the corrosion. Elevated temperature can accelerate organic matter oxidation, aging, hydrolysis, and other reactions, resulting in color deepening. Additionally, microbial action can alter the surface color of organic matter.

Acknowledgements

The authors would like to express their sincere gratitude to Professor Hui Fang of Shandong University, Researcher Chuanchang Wang and Researcher Youzhen Cai, and colleague Fenghao Wen of Shandong Cultural Relic Conservation and Restoration Center, Associate Researcher Wang Keqing of National Museum of China for their kind support and assistance in this research.

Author contributions

QM provided support and guidance for this study; YW performed all the experiments test, interpreted the data and wrote this Chinese version of the manuscript; SL wrote this English version of the manuscript; XW provided some of the samples; FL revised this manuscript. All authors read and approved the final manuscript.

Funding

This research is funded by the Humanities and Social Sciences Foundation of Shandong Province, China (Grant No. 2022-JCLS-05).

Availability of data and materials

The datasets used during this study are available from the corresponding author on reasonable request.

Declarations

Competing interests

The authors declare that they have no competing interests.

Received: 1 November 2023 Accepted: 15 April 2024
Published online: 03 May 2024

References

1. Chase WT, Franklin UM. Early Chinese black mirrors and pattern-etched weapons. Ars Orientalis Ann Arbor, 1979:215–258.
2. Karlbeck O. Notes on some early Chinese bronze mirror. China J Sci Arts. 1926;4(01):4.
3. Getten RJ. Some observations concerning the lustrous surface on certain ancient eastern bronze mirrors. Techn Stud Field Fine Arts. 1934;03:29–37.
4. Yetts WP. Problems of Chinese bronzes. J Royal Centr Asian Soc. 1931;18(03):399–402.
5. Collins WF. The mirror-black and" quicksilver" patinas of certain Chinese bronzes. J Royal Anthropol Insti Great Br Ireland. 1934;64:69–79.

6. Zhu SK, He TK. Studies of ancient Chinese mirrors and other bronze artefacts. Metal Plat Patinat. 1993:50–62.
7. Chen YY, Huang YL, Yang YN, et al. Simulation on the black lacquer patina of ancient bronze. Archaeology. 1987;02:175–8 (**(in Chinese)**).
8. He TK. Study on surface transparent layer of ancient bronze mirror. Stud Hist Nat Sci. 1985;03:251–7 (**(in Chinese)**).
9. He TK. Analysis of several black surface bronze mirrors. Acta Archaeological Sinica. 1987;01:119–31 (**(in Chinese)**).
10. Meeks ND. Tin-rich surfaces on bronze–some experimental and archaeological considerations. Archaeometry. 1986;28(02):133–62.
11. Meeks ND. Patination phenomena on Roman and Chinese high-tin bronze mirrors and other artefacts. Metal Plat Patinat. 1993: 63–84.
12. Sun SY, Ma ZZ, Jin LJ, et al. Effect of humic acid in the soil on the surface of "black patina" of bronze mirror. Cultural Relics. 1992;12:79–89 (**(in Chinese)**).
13. Ma Z, Du L, Yin X, et al. Structure and Formative Mechanism of Black Patina on Bronze Mirrors. J Univer Sci Technol Beijing. 1998;5(3):147–55.
14. Zhaozeng MA, Lianji JI, Xiulan YI. Formation of Black Patina on Bronze Mirrors Caused by Multiphenol. J Univ Sci Technol Beijing. 1997;4(2):43–6.
15. Taube M, King A H, Chase T C. Investigation of the Altered Layer on Ancient Chinese Bronze Mirrors and Model High-Tin Bronzes. MRS Online Proceeding Library Archive, 1996, 462
16. Sun HF, Niu ZR, Wang CM, et al. Scientific analysis of an ancient bronze mirror dating of Han Dynasty. Adv Mater Res. 2011;337:743–6.
17. Li BJ, Jiang XD, Wu RC, et al. Formation of black patina on an ancient Chinese bronze sword of the Warring States Period. Appl Surf Sci. 2018;455:724–8.
18. Wang YP, Liu FZ, Wang CC, Ma QL. A new understanding of the phase composition and etching evolution mechanism of tremolite. Sci Conserv Archaeol. 2020;32(06):1–12 (**(in Chinese)**).
19. Hiroshi I. Casting: Origins and history of technology. Tokyo: Industrial Technology Center of Japan, 1977.
20. Yang Y, Bai YX. On mirror moulds from the Linzi city site of the Qi State and the mirror-casting technique of the Han Period. Cultural Relics Centr China. 2020;01:102–15 (**(in Chinese)**).
21. Quanyu W, Yazheng W, Naidong L, et al. Identification of surface coatings on ceramic bronze-casting moulds from the Houma foundry, Shanxi China. J Archaeol Sci Reports. 2023;48:103858.
22. Tétreault J, Cano E, Van Bommel M, et al. Corrosion of copper and lead by formaldehyde, formic and acetic acid vapours. Stud Conservat. 2003;48(4):237–50.
23. Luo M, Guan P, Liu WH, et al. Raman spectrometry of several saturated fatty acids and their salts. Spectr Spectr Analys. 2006;26(11):2030–4 (**(in Chinese)**).
24. Ke YK, Dong HR. Handbook of analytical chemistry (3B): molecular spectroscopy. Beijing: Chemical Industry Press; 2016. (**(in Chinese)**).

Publisher's Note